Bull. Astron. Belgrade № 156 (l997), 21 – 26

UDC 521.11;523.2
Original scientific paper

THE SCHWARZSCHILD PROBLEM: A MODEL FOR THE MOTION IN THE SOLAR SYSTEM

V. MIOC and M. STAVINSCHI

Astronomical Institute of the Romanian Academy,
Str. Cutitul de Argint 5, RO-75212, Bucharest 28, Romania

(Received: July 30, 1997)

SUMMARY: The motion in a field featured by a force function $A/r + B/r^3$ (the Schwarzschild problem) constitutes a realistic model for the dynamics in the relativistic solar gravitational filed. A qualitative study is performed by using the powerful tool of McGehee's transformations. The local flow on collision and infinity manifolds is described, allowing the study of orbits with very large eccentricities. For the case of parabolic-type motion, the global flow can be described. This qualitative analysis is very useful to the understanding of the motion of certain small bodies of the solar system (comets, some asteroids) at very small and very large distances from the Sun.

1. INTRODUCTION

Consider a potential field featured by a force function

$$U(\mathbf{r}) = A/r + B/r^3, \tag{1}$$

where $\mathbf{r}$ = radius vector of a particle with respect to the source of the field, $r = |\mathbf{r}|$, A, B = real, nonzero constants. The two-body problem (or the equivalent central force problem) associated to such a field will be called *the Schwarzschild problem*. Indeed, using Schwarzschild's (1916) metric to caracterize the gravitational field, one is led to a Binet-type equation in which the force corresponds to a potential of the form (1).

The Schwarzschild problem constitutes a model for many concrete astronomical situations in the solar system: the relativistic gravitational field of Schwarzschild ($A > 0$, $B > 0$), the photogravitational field of the Sun (where situations with $A < 0$ may occur), the motion in the equatorial plane of oblate bodies ($B < 0$), etc. (see e.g. Tisserand 1889; Eddington 1923; Saari 1974; Saslaw 1978; Blaga and Mioc 1992; Stoica and Mioc 1997).

Quantitative studies on the motion in such fields were performed by many authors (e.g. Brumberg 1972; Chandrasekhar 1983; Damour and Schaefer 1986). As to qualitative studies, these ones are rather few (e.g. Saari 1974; Belenkii 1981; Szebehely and Bond 1983; Cid et al. 1983; Stoica and Mioc 1997).

This paper tackles the Schwarzschild problem from a qualitative standpoint. Resorting to the powerful tool of McGehee's (1974) transformations of the second kind, the singularity at $r = 0$ is blown up, obtaining on the one hand regularized equations of motion and integral of energy, and extending on the other hand the phase space to the *collision manifold* M_0. We describe the (fictious) flow on M_0, which provides informations about near-collisional orbits.

Next, in a somewhat symmetrically maner, we build the so-called *infinity manifold* M_∞, and describe the flow on it. This is a fictious flow again, but

allows the understanding of the behaviour of near-escape motion.

Finally, exploiting the rotational symmetry of the global flow, we reduce the 4D full phase space to dimension 3. Considering the angular momentum to be a check parameter, clear pictures of the global flow can be obtained in the zero energy case. The reduced phase space structure is described for the whole interplay among the field parameter and the angular momentum. The phase curves are both transposed in full phase space and interpreted in terms of physical motion.

Of course, the zero energy case constitutes a rather special situation among the motion in the solar system. Neverthless, there are orbits of certain bodies (comets, some asteroids, grains, dust) related to such a case. The Schwarzschild model allows a better understanding of the behaviour of very eccentric trajectoires at very small and very large distances from the central body.

2. EQUATIONS OF MOTION AND FIRST INTEGRALS

The potential (1) is central, hence the motion is planar. Let the field source be fixed at the origin of the motion plane $\mathbf{R}^2$, and let $\mathbf{q} = (q_1, q_2) \in \mathbf{R}^2$, $\mathbf{p} = (p_1, p_2) \in \mathbf{R}^2$ be the configuration and the momentum vector of the moving body (hereafter particle), respectively. The motion equations read

$$\begin{cases} \dot{\mathbf{q}} = \partial H(\mathbf{q}, \mathbf{p})/\partial \mathbf{p}, \\ \mathbf{p} \doteq -\partial H(\mathbf{q}, \mathbf{p})/\partial \mathbf{q}, \end{cases} \tag{2}$$

and define a vector field on the phase space $\mathbf{Q} \times \mathbf{P}$, where $\mathbf{Q} = \mathbf{R}^2 \backslash \{(0,0)\}$ is the configuration space, while $\mathbf{P} = \mathbf{R}^2$ is the momentum space. The Hamiltonian

$$H(\mathbf{q}, \mathbf{p}) = |\mathbf{p}|^2/2 - A/|\mathbf{q}| - B/|\mathbf{q}|^3 = h/2, \tag{3}$$

is a first integral of the motion (the energy integral; h is the energy constant). Another first integral is that of angular momentum

$$L(\mathbf{q}, \mathbf{p}) = q_1 p_2 - q_2 p_1 = C, \tag{4}$$

where C is the angular momentum constant.

3. McGEHEE'S TRANSFORMATIONS

The potential, the energy integral, and the equations of motion have an isolated singularity at the origin: $\mathbf{q} = (0,0)$; it corresponds to the collision of the particle with the centre (see Saari 1974). To remove it, we apply successively the McGehee (1974) transformations of the second kind:

$$\begin{cases} r = |\mathbf{q}|, \\ \theta = \arctan(q_2/q_1), \\ u = \dot{r} = (q_1 p_1 + q_2 p_2)/|\mathbf{q}|, \\ v = r\dot{\theta} = (q_1 p_2 - q_2 p_1)/|\mathbf{q}|; \end{cases} \tag{5}$$

$$\begin{cases} x = r^{3/2} u, \\ y = r^{3/2} v; \end{cases} \tag{6}$$

$$dt = r^{5/2} ds. \tag{7}$$

These steps (which all define real analytic diffeomorphisms) perform the following changes: (5) introduce the standard polar coordinates, (6) scale down the polar components of the velocity, while (7) rescales the time. Under transformations (5)-(7), the equations of motion become (Stoica and Mioc 1997)

$$\begin{cases} r' = rx, \\ x' = \dfrac{3x^2}{2} + y^2 - Ar^2 - 3B, \\ \theta' = y, \\ y' = \dfrac{xy}{2}, \end{cases} \tag{8}$$

with $' = d/ds$. The first integrals (3) and (4) now read

$$x^2 + y^2 = hr^3 + 2Ar^2 + 2B; \tag{9}$$

$$y^2 = C^2 r. \tag{10}$$

Equations (8)-(10) are well defined for the boundary $r = 0$. This means that the phase space of the vector field (8) can be extended analytically to this boundary, which is invariant under the flow because $r' = 0$ when $r = 0$. The energy and angular momentum relations (9) and (10) also extend smoothly to the boundary $r = 0$.

4. COLLISION MANIFOLD

Let us denote

$$E_h = \{(r, \theta, x, y) \mid x^2 + y^2 = hr^3 + 2Ar^2 + 2B\}, \tag{11}$$

$$M_{col} = \{(r, \theta, x, y) \mid r = 0\}, \tag{12}$$

and define the *collision manifold* as $M_0 = E_h \cap M_{col}$. In other words,

$$M_0 = \{(r, \theta, x, y) \mid r = 0; \theta \in S^1; x^2 + y^2 = 2B\}. \tag{13}$$

Obviously, for $B > 0$, M_0 is a 2D cylinder (or a 2D torus, since $\theta \in S^1$) in the 3D space of the coordinates (θ, x, y), actually imbedded in the 4D full phase space of the coordinates (r, θ, x, y). For $B = 0$, M_0 reduces to the circle $\{r = 0; \theta \in S^1; x = y = 0\}$, whereas, for $B < 0$, $M_0 = \emptyset$, namely collisions cannot occur, as Saari (1974) already proved, but within another framework and resorting to another method. Remark that for $M_0 \neq \emptyset$ ($B \geq 0$) every energy level shares the boundary $r = 0$ (since M_0 does not depend on h).

The flow on M_0 has no physical signifiance; however, due to the continuity of solutions with respect to initial data, this fictious flow provides valuable informations about the near-collisional orbits. The vector field on M_0 is given by

$$\begin{cases} \theta' = y, \\ x' = -\dfrac{y^2}{2}, \\ y' = \dfrac{xy}{2}. \end{cases} \tag{14}$$

There are two circles of equilibria on the M_0 torus: $(\theta, x, y) = (\theta \in S^1, \pm\sqrt{2B}, 0)$. One sees by the second equation (14) that $x' < 0$ for $y \neq 0$, therefore, besides the degenerate equilibria at $y = 0$, the flow consists only of heteroclinic orbits moving from the *upper circle* (UC) $x = \sqrt{2B}$ to the *lower circle* (LC) $x = -\sqrt{2B}$. To deduce the slope of these orbits, one puts $x = \sqrt{2B}\sin\alpha$, $y = -\sqrt{2B}\cos\alpha$, leading to $d\alpha/d\theta = 1/2$. The flow on M_0 (considered as a cylinder) is illustrated in Figure 1.

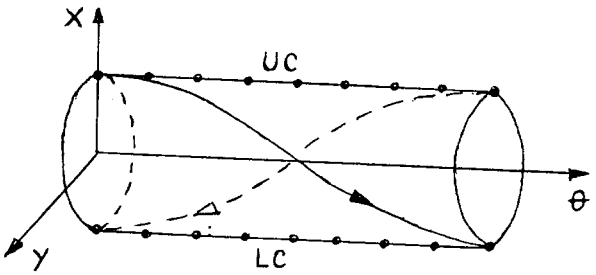

Fig. 1. *The flow on the M_0 cylinder.*

Remark that collisions can occur not only for rectilinear motion ($C = 0$), but for $C \neq 0$, too (see also Saari 1974; McGehee 1981). In this last case, writing the angular momentum integral in polar coordinates, one sees that $\dot\theta \to \infty$ when $r \to 0$, which means that the particle spirals infinitely many times around the centre immediately before collision (after ejection). This is the so-called *black hole effect* (Diacu et al. 1995).

As a last remark, by (10) it is clear that all collisional orbits tend to LC or eject from UC.

5. INFINITY MANIFOLD

Somewhat symmetrically, let us tackle the so-called *infinity manifold*, corresponding to $r \to \infty$. For this purpose we apply successively the transformations (Mioc and Stoica 1997)

$$\rho = 1/r; \tag{15}$$

$$\begin{cases} \xi = \rho^{3/2} x, \\ \eta = \rho^{3/2} y; \end{cases} \tag{16}$$

$$ds = \rho^{3/2} d\tau, \tag{17}$$

which all are real analytic diffeomorphisms. Under them, the motion equations turn into

$$\begin{cases} d\rho/d\tau = -\rho\xi, \\ d\theta/d\tau = \eta, \\ d\xi/d\tau = \eta^2 - A\rho - 3B\rho^3, \\ d\eta/d\tau = -\xi\eta, \end{cases} \tag{18}$$

while the first integrals (9) and (10) become respectively

$$\xi^2 + \eta^2 = h + 2A\rho + 2B\rho^3; \tag{19}$$

$$\eta = C\rho. \tag{20}$$

Denote

$$\tilde E_h = \{(\rho, \theta, \xi, \eta) \mid \xi^2 + \eta^2 = h + 2A\rho + 2B\rho^3\}, \tag{21}$$

$$M_{\inf} = \{(\rho, \theta, \xi, \eta) \mid \rho = 0\}, \tag{22}$$

and define the *infinity manifold* as $M_\infty = \tilde E_h \cap M_{\inf}$, that is

$$M_\infty = \{(\rho, \theta, \xi, \eta) \mid \rho = 0; \theta \in S^1; \xi^2 + \eta^2 = h\}. \tag{23}$$

It is clear that, for $h > 0$, M_∞ is a 2D cylinder (or a 2D torus, because $\theta \in S^1$) in the 3D space of the coordinates (θ, ξ, η), actually imbedded in the 4D space of the coordinates $(\rho, \theta, \xi, \eta)$. For $h = 0$, M_∞ reduces to the circle $\{\rho = 0; \theta \in S^1; \xi = \eta = 0\}$, while $h < 0$ leads to $M_\infty = \emptyset$. In other words, for $h < 0$ the particle cannot escape.

The flow on M_∞ has no more physical signifiance than that on M_0. Nevertheless, due to the same continuity with respect to initial data, this fictious flow contributes to a better understanding of the behaviour of near-escape orbits. The vector field on M_∞ is given by

$$\begin{cases} d\theta/d\tau = \eta, \\ \xi/d\tau = \eta^2, \\ d\eta/d\tau = -\xi\eta. \end{cases} \tag{24}$$

There are two circles of equilibria on the M_∞ torus: $(\theta, \xi, \eta) = (\theta_0 \in S^1, \pm\sqrt{h}, 0)$. The second equation (24) shows that $d\xi/d\tau > 0$ for $\eta \neq 0$, that is, the remainder of the flow on M_∞ (leaving aside the degenerate equilibria at $\eta = 0$) consists of heteroclinic orbits moving from the *lower circle* (LC) $\xi = -\sqrt{h}$ to the *upper circle* (UC) $\xi = \sqrt{h}$. To determine the slope of these phase curves, put $\xi = \sqrt{h}\sin\alpha$, $\eta = -\sqrt{h}\cos\alpha$, which yields $d\alpha/d\theta = -1$. The flow on M_∞ (considered as a cylinder) is illustrated in Figure 2.

By (20), it is obvious that all orbits neighbour infinity in the zone of UC (the outwards moving ones) or LC (those which move inwards). It is also clear that the coordinates (ξ, η) are nothing but the polar components of the velocity (u, v). In addition, the vector field (18) could be derived directly from the initial equations of motion. Neverthless, the elegance of McGehee's transformations made us to choose this way to obtain equations (18)-(20).

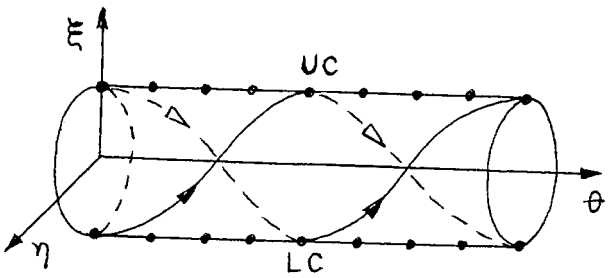

Fig. 2. *The flow on the M_∞ cylinder.*

As a final remark, taking into account (7), (15), and (17), the flows on M_0 and M_∞ constitute equilibria for the phase space orbits.

6. ZERO ENERGY GLOBAL FLOW

Since θ does not appear explicitly in (8) and (9), we can reduce the 4D full phase space to dimension 3 (obtaining the reduced phase space RPS) by factorizing the flow to S^1. In RPS the M_0 torus becomes the circle $\{r = 0; \}x^2+y^2 = 2B\}$ whose points M torus.

Considering the energy to be a parameter, we approach here the zero energy case ($h = 0$), for which we are able to obtain clear pictures of the global flow. By (8) and (9), the vector field in RPS reads in this case

$$\begin{cases} r' = rx, \\ x' + \dfrac{x^2}{2} + Ar^2 - B, \\ y' = \dfrac{xy}{2}, \end{cases} \tag{25}$$

while the energy relation becomes

$$x^2 + y^2 - 2Ar^2 = 2B. \tag{26}$$

The last relation shows that in RPS the zero energy level is a quadric surface foliated by the first integral (10) into curves lying on a parabolic cylinder ($C \neq 0$) or in the plane $y = 0$ (if $C = 0$). In full phase space, every such orbit is actually a manifold consisting of the product between the RPS orbit and S^1.

For $A > 0$, $B > 0$, (26) represents the upper "half" of a hyperboloid of one sheet, whose "equator" is the M_0 circle (Figure 3). If $C = 0$, we have the two branches of hyperbola 1; if $0 < C^2 < 4\sqrt{AB}$, we have the orbits 2. In full phase space they are ty

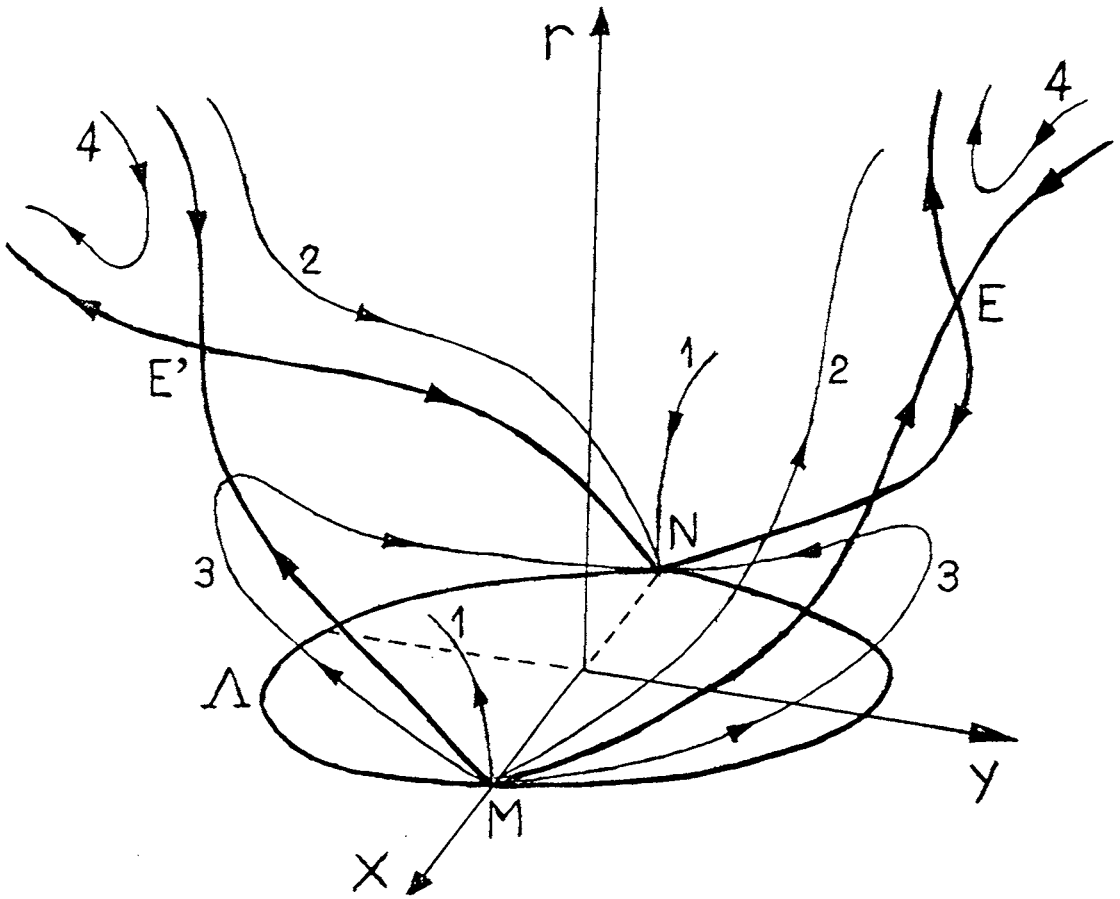

Fig. 3. *The global flow for $A > 0$, $B > 0$, $h = 0$.*

or come from infinity and tend to LC. Physically speaking, they are trajectoires of the type ejection-escape or infinity-collision, rectilinear (curves 1) or not; for curves 2 the particle spirals infinitely many times around the centre before collision (after ejection). The asymptotic velocity at infinity is zero (as in all similar cases below).

If $C^2 = 4\sqrt{AB}$, the solutions in RPS are the two separatrices with their saddles located at . E $(\sqrt{B/A}, 0, \sqrt{2B})$, E' $(\sqrt{B/A}, 0, -\sqrt{2B})$. They correspond in full phase space to circles, and in physical space to unstable circular motion at distance $r = \sqrt{B/A}$ from the centre. The heteroclinic lower branches of the separatrices are in full phase space heteroclinic solutions ejecting from UC and tending asymptotically to unstable circular motion (for ME, ME'), or conversely (for EN, E'N). As to the upper branches of the separatrices, they are in full phase space solutions that come from infinity and tend asymptotically to unstable circular motion, or conversely. The corresponding physical motion consists of spirals which behave similarly.

If $C^2 > 4\sqrt{AB}$, the orbits in RPS are curves 3 ($r < \sqrt{B/A}$) or 4 ($r > \sqrt{B/A}$). The heteroclinic curves 3 are in full phase space heteroclinic orbits connecting UC with LC. Physically, they are trajectories that eject spiralling from collision and end spiralling in collision. Curves 4 represent in both full phase space and physical space noncolliding orbits which come from infinity and then tend back to infinity.

For $A < 0$, $B > 0$, (26) represents the upper half of an ellipsoid, its equator being the M_0 circle (Figure 4). All orbits are heteroclinic; in full phase space they represent heteroclinic solutions which connect UC with LC. In physical terms, we deal with bounded motions that start and end in collision. The particle moves radially if $C = 0$ (curve 1) or spirals at ejection (collision) else.

For $A > 0$, $B < 0$, the motion is collisionless. According to (26), the zero energy level in RPS is the upper sheet of a hyperboloid of two sheets (Figure 5). In full phase space, all solutions are of infinity-infinity type. The physical orbits come from infinity, reach a minimum distance, and then escape back to infinity. The motion is radial if $C = 0$ (curve 1), or spiral else.

For $A < 0$, $B < 0$, (26) shows that zero energy level in RPS is an imaginary ellipsoid, hence the

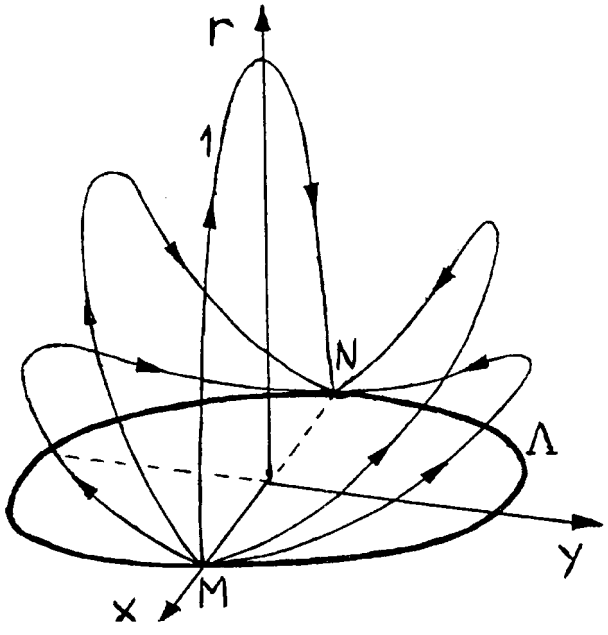

Fig. 4. *The global flow for $A < 0$, $B > 0$, $h = 0$.*

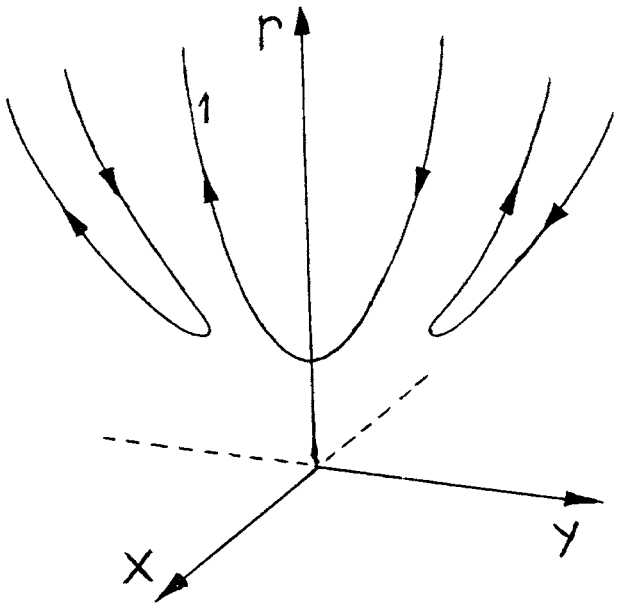

Fig. 5. *The global flow for $A > 0$, $B < 0$, $h = 0$.*

REFERENCES

Belenkii, I.M.: 1981, *Celest. Mech.* **23**, 9.
Blaga, P., Mioc, V.: 1992, *Europhys. Lett.* **17**, 275.
Brumberg, V.A.: 1972, *Relativistic Celestial Mechanics*, Nauka, Moscow (Russian).
Chandrasekhar, S.: 1983, *The Mathematical Theory of Black Holes*, Oxford University Press, Oxford.
Cid, R., Ferrer, S., Elipe, A.: 1983, *Celest. Mech.* **31**, 73.
Damour, T., Schaefer, G.: 1986, *Nuovo Cimento* **101B**, 127.
Diacu, F.N., Mingarelli, A., Mioc, V., Stoica, C.: 1995, in R.P.Agarvwal (ed.), *Dynamical Systems and Applications*, World Scientific Series in Applicable Analysis, Vol. **4**, World Scientific, Singapore, 213.
Eddington, A.S.: 1923, *Mathematical Theory of Relativity*, Cambridge University Press, Cambridge.

McGehee, R.: 1974, *Invent. Math.* **27**, 191.
McGehee, R.: 1981, *Comment. Math. Helvetici* **56**, 524.
Mioc, V., Stoica, C.: 1997, *Rom. Astron. J.* **7**, 19.
Saari, D.G.: 1974, *Celest. Mech.* **9**, 55.
Saslaw, W.C.: 1978, *Astrophys.J.* **226**, 240.
Schwarzschild, K.: 1916, *Sitzber. Preuss. Akad. Wiss. Berlin*, 189.
Stoica, C., Mioc, V.: 1997, *Astrophys. Space Sci.* **249**, 161.
Szebehely, V., Bond, V.: 1983, *Celest. Mech.* **30**, 59.
Tisserand, F.: 1989, *Traité de Mécanique Céleste*, Gauthier-Villars, Paris.

ШВАРЦШИЛДОВ ПРОБЛЕМ: ЈЕДАН МОДЕЛ ЗА КРЕТАЊЕ У СУНЧЕВОМ СИСТЕМУ

В. Миок и М. Ставински

Astronomical Institute of the Romanian Academy,
Str. Cutitul de Argint 5, RO-75212, Bucharest 28, Romania

УДК 521.11;523.2
Оригинални научни рад

Кретање у пољу окарактерисаном функцијом силе $A/r + B/r^3$ (Шварцшилдов проблем) конституише један реалан модел за динамику у релативистичком Сунчевом пољу гравитације. Квалитативно проучавање се обавља уз помоћ моћног алата као што су Мек Гехијеве трансформације. Многострукости локалног тока судара и бесконачности се описују проучавањем путања са врло великим ексцентричностима. Глобални ток може да се опише у случају путања параболичног типа. Ова квалитативна анализа је врло корисна за разумевање кретања одређених малих тела Сунчевог система (комете, неки астероиди) на врло малим и врло великим растојањима од Сунца.